Electronic Supplementary Material (ESI) for Inorganic Chemistry Frontiers.

Supporting Information

Chiral defect induced blue photoluminescence and circular polarization luminescence of zero-dimensional Cs_4PbBr_6 perovskite nanocrystals

*Jiaqi Zhao[1], Yuan Wang[1], Tinglei Wang[1] and Yu Wang[1]**

[1] State Key Laboratory of Inorganic Synthesis and Preparative Chemistry, College of Chemistry, Jilin University, 2699 Qianjin Street, Changchun 130012

*Corresponding Authors: wangyu@jlu.edu.cn.

Table of Contents

1. Schematic illustrations of the crystal structures

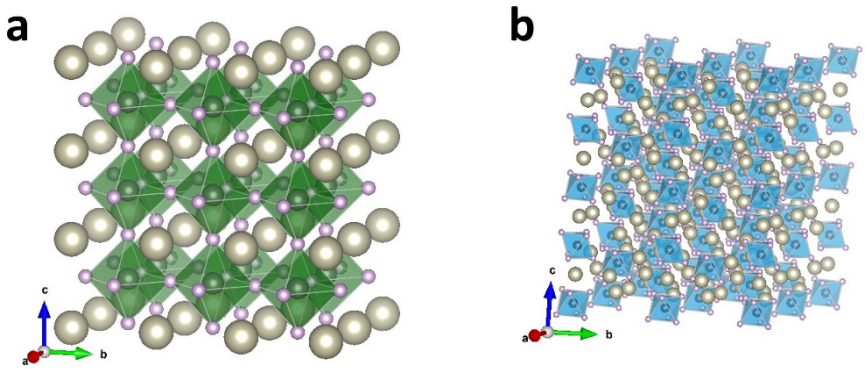

Fig. S1. Schematic illustrations of the crystal structures of (a) three-dimensional (3-D) cubic phase $CsPbBr_3$ and (b) zero-dimensional (0-D) rhombohedral phase Cs_4PbBr_6.

2. TEM and HRTEM images of $CsPbBr_3$ NCs

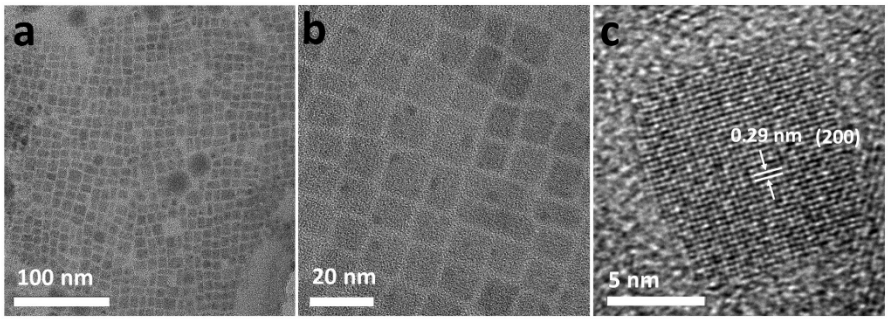

Fig. S2. TEM images of (a, b) $CsPbBr_3$ NCs with different magnifications. HRTEM images of $CsPbBr_3$ NCs.

3. XRD patterns of $CsPbBr_3$ NCs

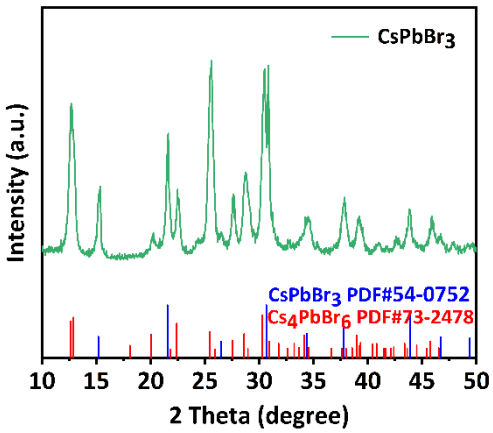

Fig. S3. XRD patterns of $CsPbBr_3$ NCs.

4. UV−vis spectra and PL spectra of $CsPbBr_3$ NCs

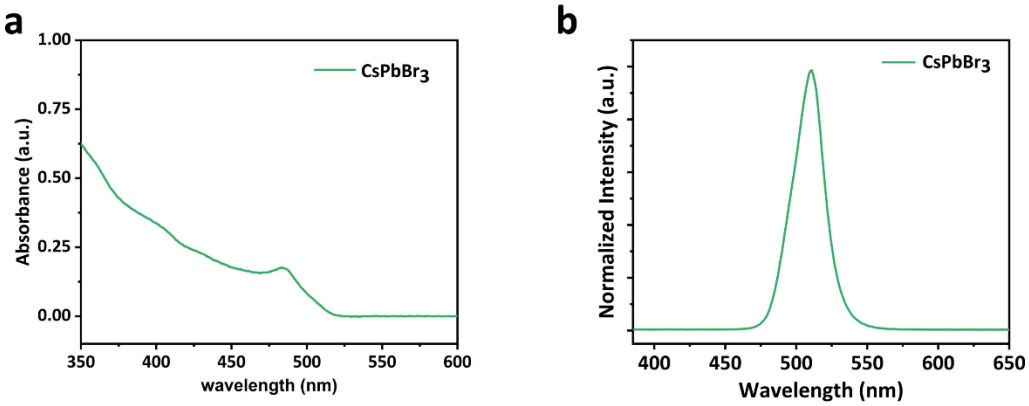

Fig. S4. (a) UV−vis spectra and (b) PL spectra of $CsPbBr_3$ NCs.

5. Particle size distribution of *R*-, *S*-Cs_4PbBr_6 NCs

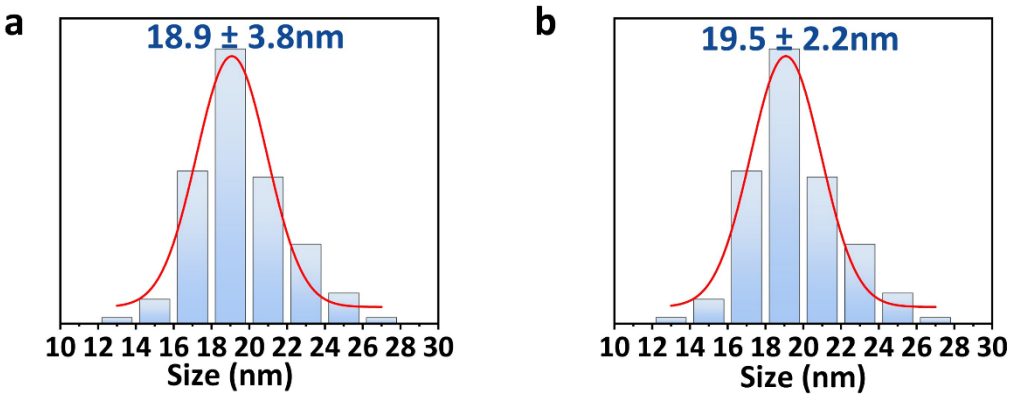

Fig. S5. Particle size distribution of *R*-, *S*-Cs_4PbBr_6 NCs.

6. HRTEM image and selected-area FFT patterns

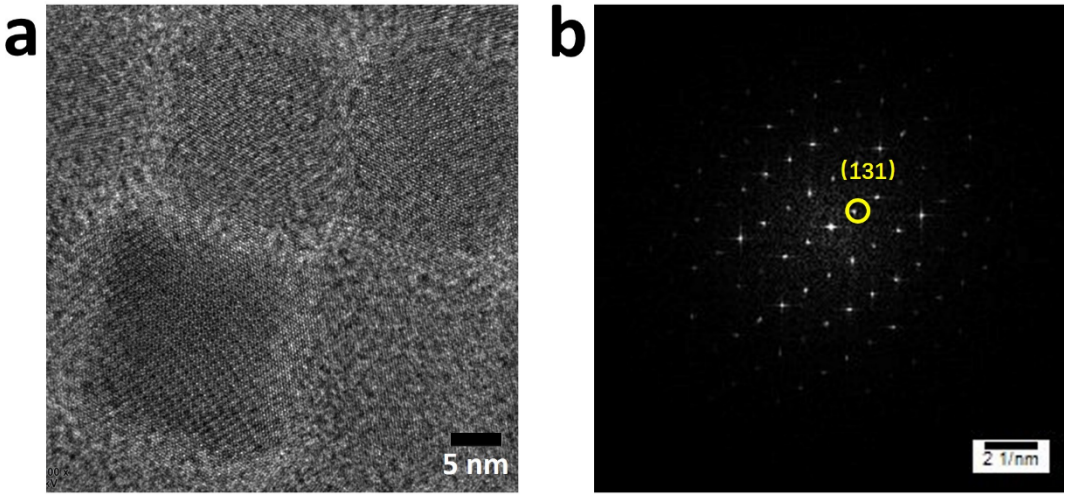

Fig. S6. HRTEM image of a) *R*-Cs_4PbBr_6 NCs and b) the corresponding selected-area FFT patterns.

7. TEM and HRTEM images of N-Cs_4PbBr_6 NCs

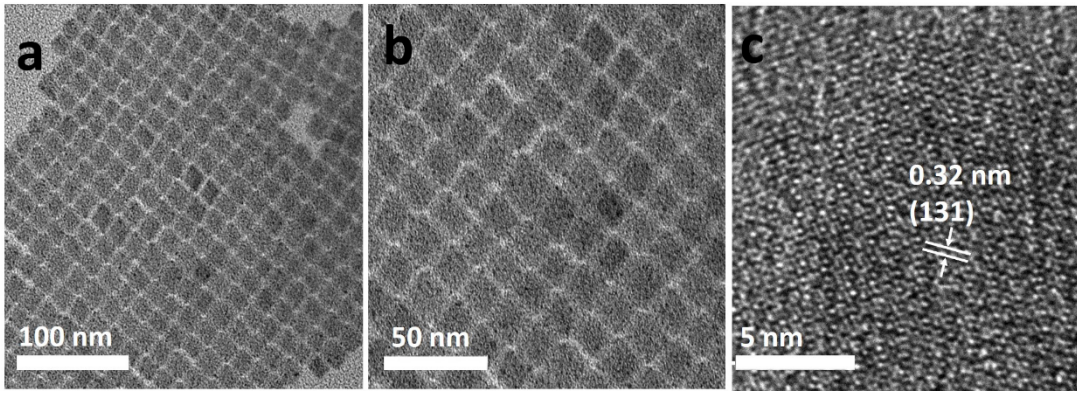

Fig. S7. TEM images of (a, b) N-Cs_4PbBr_6 NCs with different magnifications. HRTEM image of N-Cs_4PbBr_6 NCs.

8. Photographs of $CsPbBr_3$ NCs

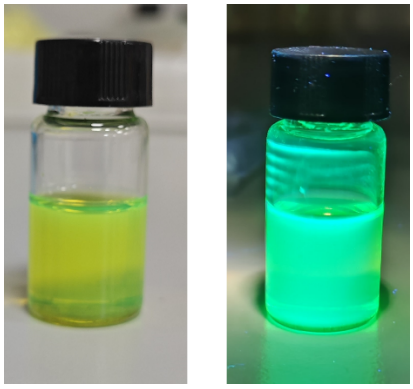

Fig. S8. Photographs of $CsPbBr_3$ NCs under visible illumination (left) and UV 365 nm illumination (right).

9. UV–vis and PL spectra of N-Cs_4PbBr_6 NCs

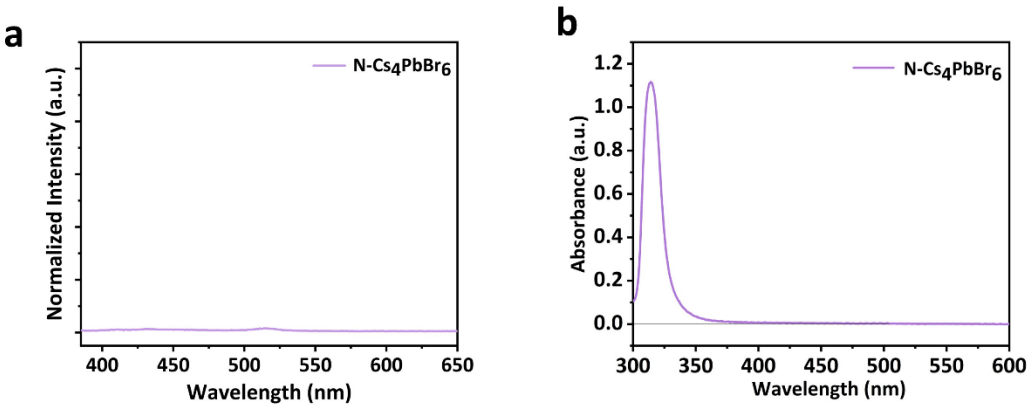

Fig. S9. (a) PL spectrum and (b) UV–vis spectrum of N-Cs_4PbBr_6 NCs.

10. Photographs of N-Cs_4PbBr_6 NCs

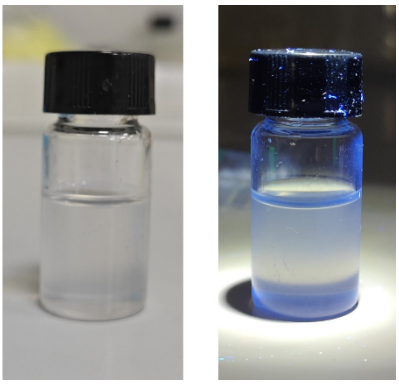

Fig. S10. Photographs of N-Cs_4PbBr_6 NCs under visible illumination (left) and UV 365 nm illumination (right).

11.PL decay lifetime of *R*-, *S*-Cs_4PbBr_6 NCs.

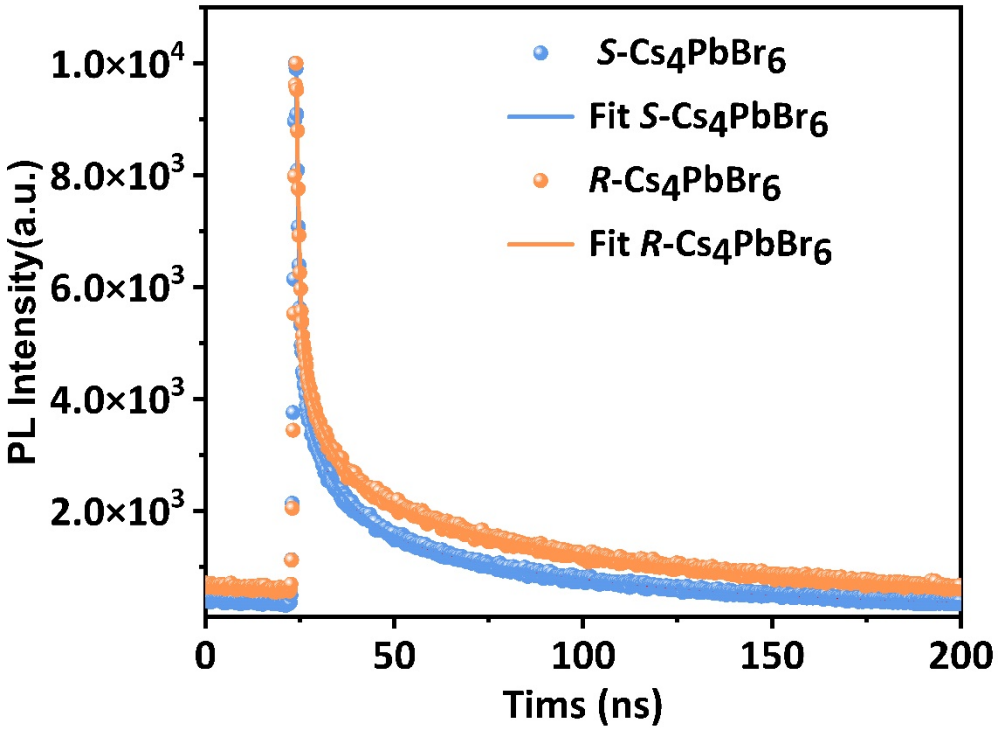

Fig. S11. PL decay lifetime of *R*-, *S*-Cs_4PbBr_6 NCs.

12.Optical band gap

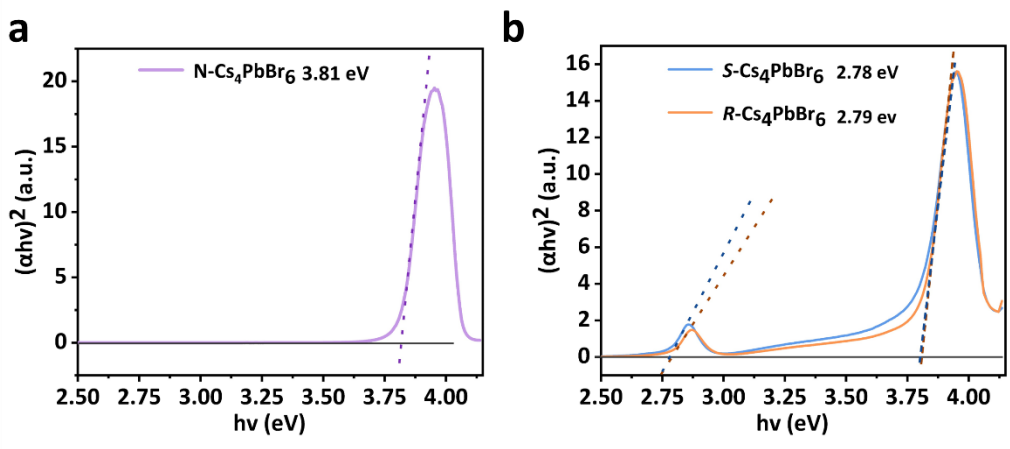

Fig. S12. Optical band gap of (a) N-Cs_4PbBr_6 NCs and (b) *R*-, *S*-Cs_4PbBr_6 NCs.

13.CD spectra

13.1. CD spectra of *R*-, *S*-MBA

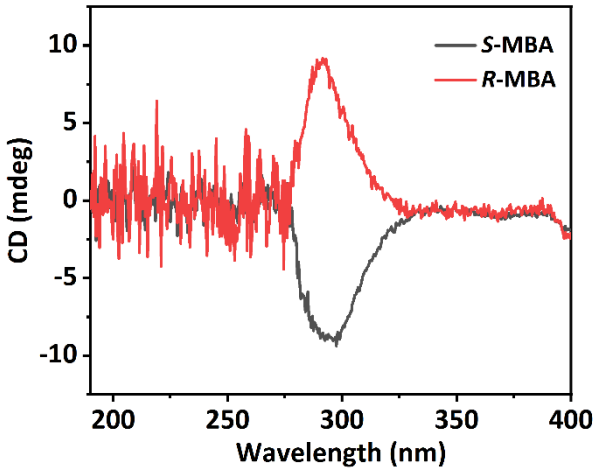

Fig. S13. CD spectra of *R*-, *S*-MBA in toluene solution.

13.2. CD spectra of $CsPbBr_3$ and N-Cs_4PbBr_6NCs

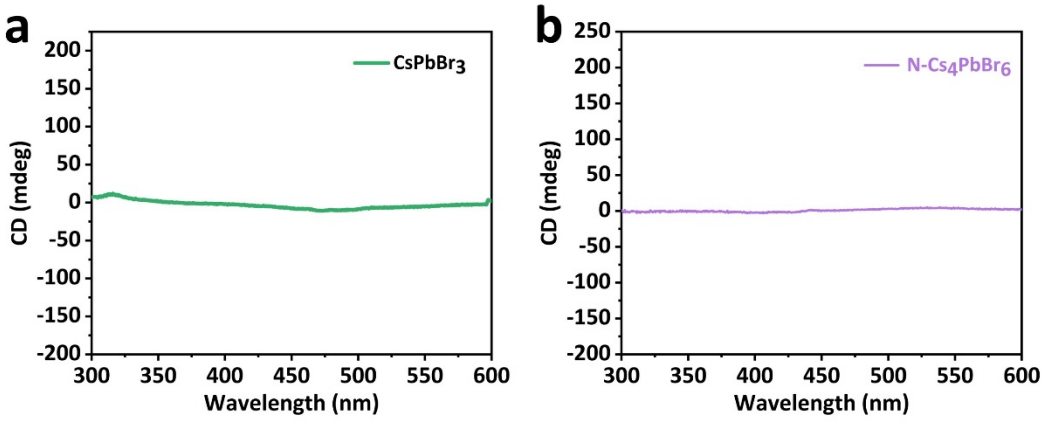

Fig. S14. CD spectra of (a) $CsPbBr_3$ and (b) N-Cs_4PbBr_6 NCs.

13.3. CD and g_{abs} spectra of $CsPbBr_3$ NCs with different content of chiral precursors solution

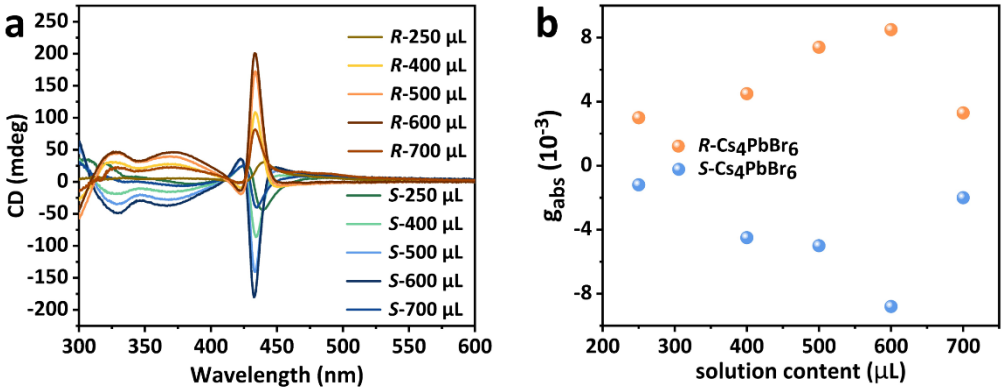

Fig. S15. CD spectra of $CsPbBr_3$ NCs with different content of chiral precursors solution and corresponding g_{abs} values.

13.4. DC (V) plots of *R*-, *S*-Cs_4PbBr_6 NCs

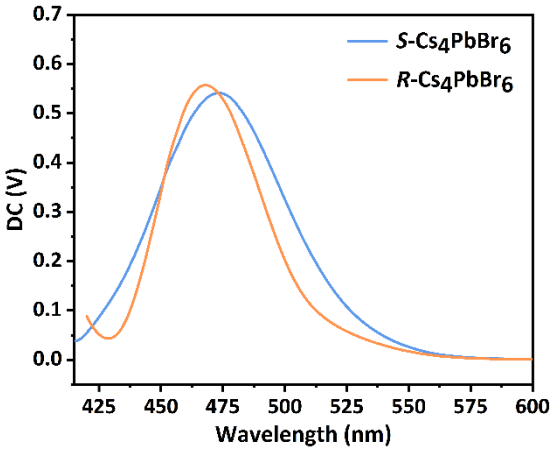

Fig. S16. DC (V) plots of *R*-, *S*-Cs_4PbBr_6 NCs.

14. TEM images of $CsPbBr_3$ NCs with different content of chiral precursors solution.

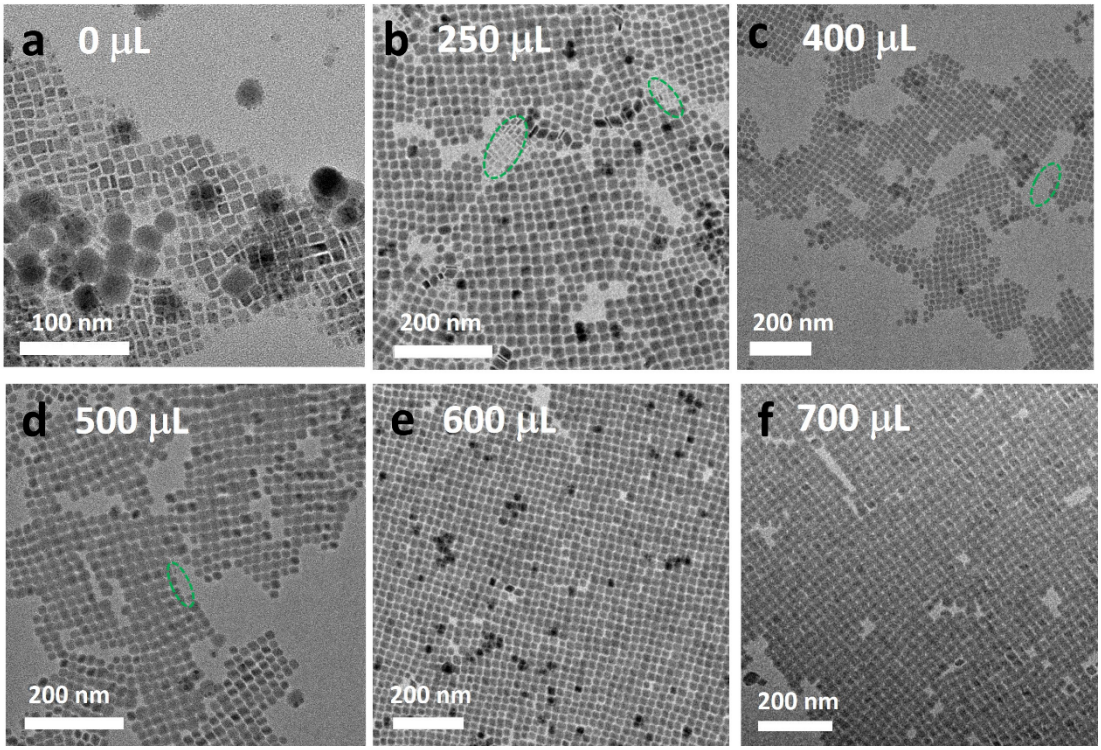

Fig. S17. TEM images of $CsPbBr_3$ NCs with different content of chiral precursors solution. The green area circled is cubic $CsPbBr_3$ NCs without phase transformation.

15.PL and UV−vis spectra of $CsPbBr_3$ NCs with different content of chiral precursors solution.

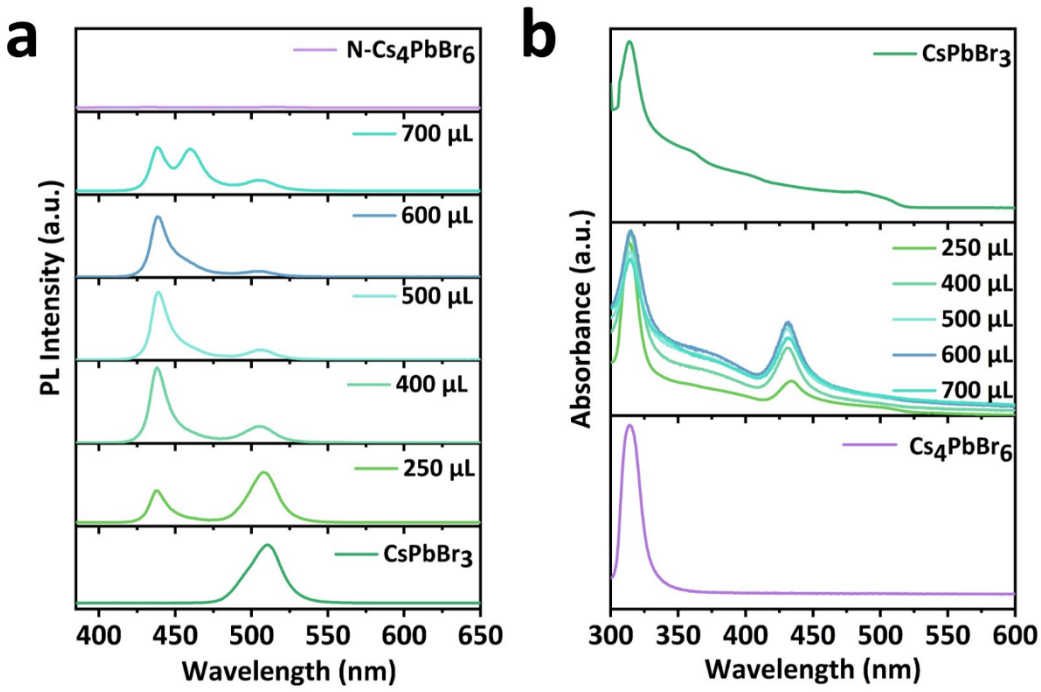

Fig. S18. The (a) PL spectra and (b) UV−vis spectra of $CsPbBr_3$ NCs with different content of chiral precursors solution.

16.XRD patterns of $CsPbBr_3$ NCs with different content of chiral precursors solution.

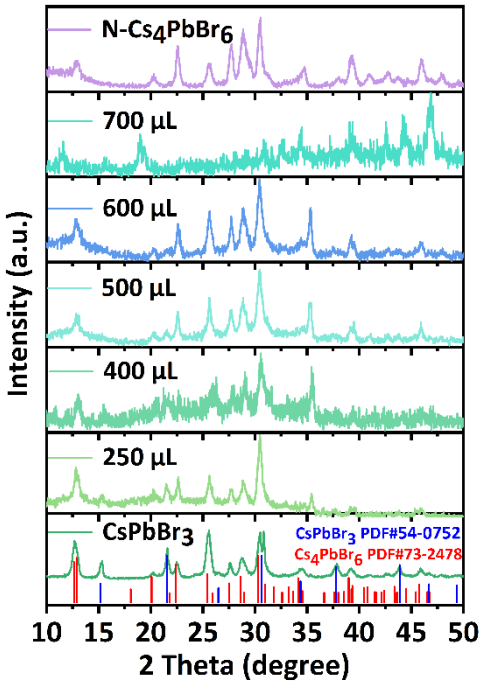

Fig. S19. XRD patterns of $CsPbBr_3$ NCs with different content of chiral precursors solution.

17.FTIR Characterization

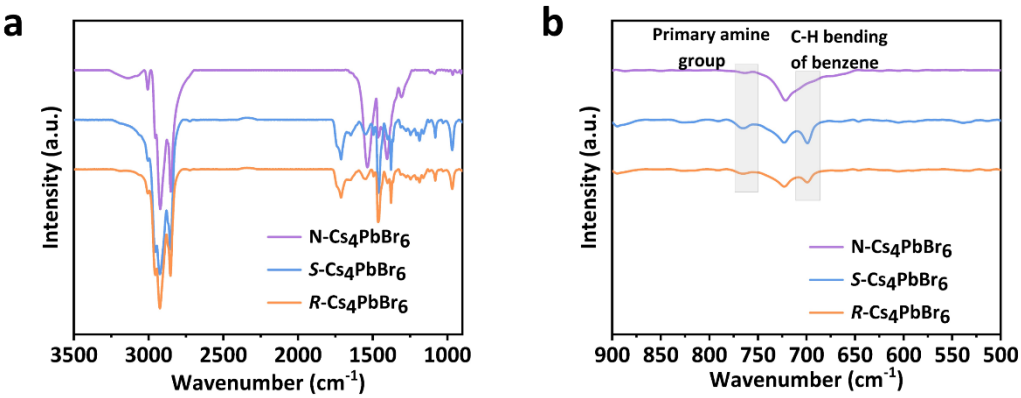

Fig. S20. The FTIR spectra of N-Cs_4PbBr_6, *R*-, *S*-Cs_4PbBr_6 NCs at different wavenumber regions.

18.XPS Analysis

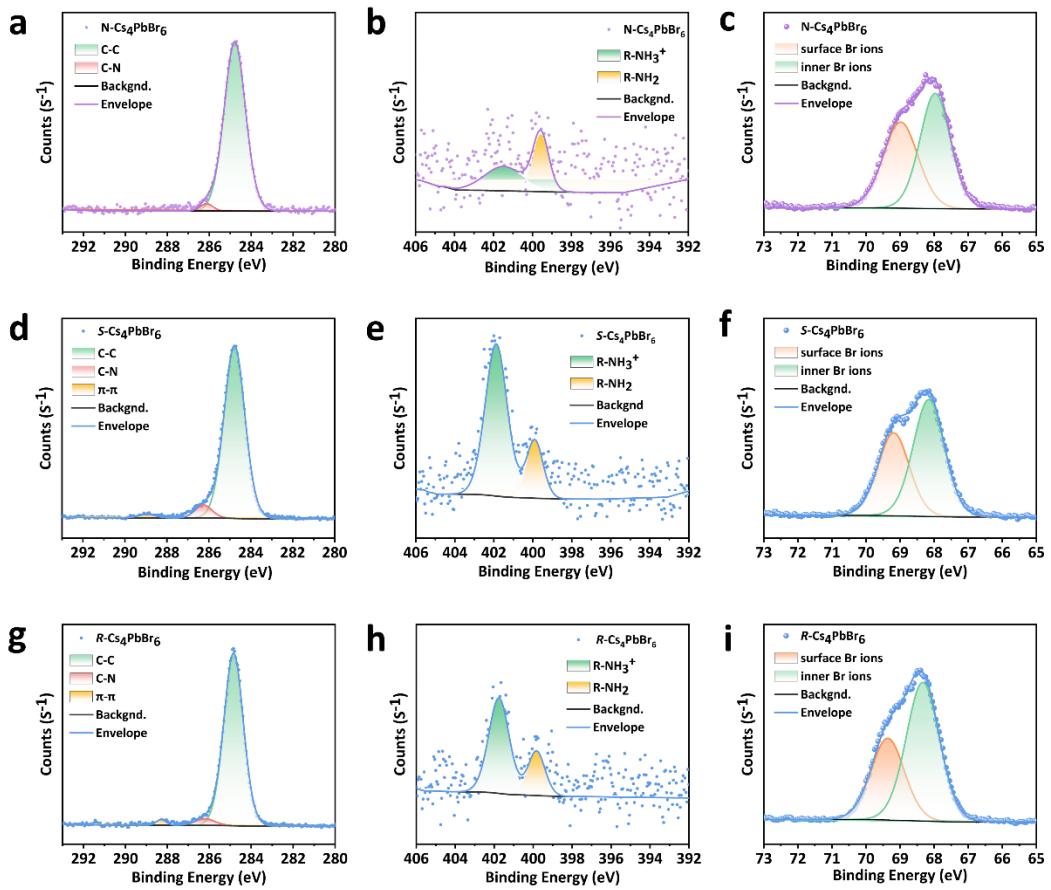

Fig. S21. XPS spectra of (a-c) N 1s, C 1s and Br of $CsPbBr_3$ NCs, (d-f) N 1s, C 1s and Br of *S*-Cs_4PbBr_6 NCs, (g-i) N 1s, C 1s and Br of *R*-Cs_4PbBr_6 NCs.

19.NMR spectra

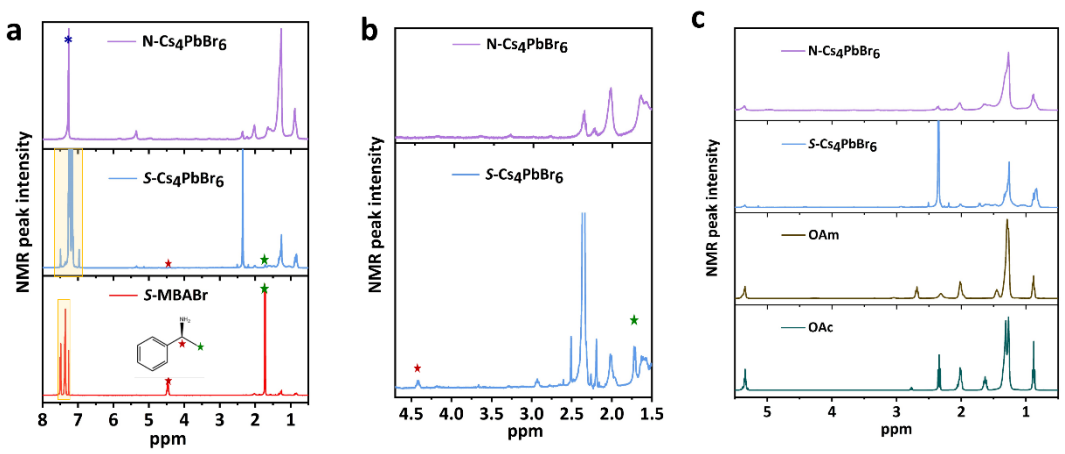

Fig. S22. ^{1}H NMR spectra of (a) N-Cs_4PbBr_6 NCs, *S*-Cs_4PbBr_6 NCs and *S*-MBABr in chloroform-d ($CDCl_3$). The blue asterisks refer to the solvent signal, the orange region is the chemical shift of ^{1}H on the benzene ring. (b)The regional magnification of ^{1}H NMR spectrum of N-Cs_4PbBr_6 NCs and *S*-Cs_4PbBr_6 NCs. (c) ^{1}H NMR spectrum of N-Cs_4PbBr_6 NCs, *S*-Cs_4PbBr_6 NCs, OAm and OAc at chemical shifts of 5.5-0.5 ppm.

20.TRPL Data

Table S1. TRPL results for *R*-, *S*-Cs_4PbBr_6 NCs.

Sample	τ_1 (ns)	A_1	τ_2 (ns)	A_2	τ_3 (ns)	A_3	τ_{ave} (ns)
S-Cs_4PbBr_6	0.9223	6.03 %	9.302	19.21 %	52.36	72.76 %	50.36
R-Cs_4PbBr_6	0.8654	7.91%	8.027	22.90%	44.24	69.20%	42.10

The films were fitted with a triexponential function of the form:

$$A(t) = A_1\exp(-t/\tau_1) + A_2\exp(-t/\tau_2) + A_3\exp(-t/\tau_3) \quad (3)$$

$$\tau_{ave} = (A_1\tau_1^2 + A_2\tau_2^2 + A_3\tau_3^2)/(A_1\tau_1 + A_2\tau_2 + A_3\tau_3) \quad (4)$$

Where, τ_1, τ_2 and τ_3 present the decay time, A_1, A_2 and A_3 present the relative contributions, respectively.

21. The absorption dissymmetry factor (g_{abs})

Table S2. The g_{abs}-factor values ($\times 10^{-3}$) of chiral *R*-, *S*-Cs_4PbBr_6 NCs treated with different content of chiral solution.

Sample	250	400	500	600	700
S-Cs_4PbBr_6	-1.2	-4.5	-5	-8.8	-2
R-Cs_4PbBr_6	3	4.5	7.4	8.5	3.3